

Preparation and Characterization of Nanostructured Electrodes by Electrophoretically Co-deposition of Pd and Pt Nanoparticles

Long-Biao Lai, Dong-Hwang Chen,* and Ting-Chia Huang

Department of Chemical Engineering, National Cheng Kung University, Tainan, Taiwan 701, ROC

(Received October 17, 2002)

A novel Pd-doped Pt/Ti nanostructured electrode was prepared by the electrophoretic co-deposition of Pt and Pd nanoparticles on a Ti support in a reverse micellar solution of water/Aerosol OT/isooctane, followed by a heat treatment in air at 400 °C. The total catalyst loading (Pt and Pd) was fixed at 0.015 mmol/cm^2, referred to the geometric area. The crystal structure, surface morphology, and elemental distribution of the resultant electrode were characterized by XRD, SEM, and SEM-WDS, respectively. The surface composition and electrocatalytic activity of the electrode were investigated by cyclic voltammetry in a solution of 0.5 M H_2SO_4 and a mixed solution of 0.1 M CH_3OH and 1.0 M NaOH, respectively. The composition on the electrode surface could be controlled by adjusting the composition of the electrodeposition solution. Also, with increasing the Pd content on the electrode surface, the electrocatalytic activity of the Pd-doped Pt/Ti nanostructured electrodes for the oxidation of CH_3OH first increased, and then decreased after reaching a maximum at a surface composition of 20 atom % Pd. When the Pd content on the electrode surface was larger than 60%, the electrocatalytic activity of the Pd-doped Pt/Ti nanostructured electrode was lower than that of the Pt/Ti electrode because most active sites were occupied by the relatively inactive Pd. This result revealed that the activity enhancement or diminution resulted from the doping of Pd in Pt at an atomic level might be achieved via the interaction between Pt and Pd nanoparticles. In addition, at a surface composition of 20 atom % Pd, the current density at 25 °C was 55 mA/cm^2, revealing that the resultant electrode had a rather high current density and specific activity.

It is known that Pt is the most active catalyst for hydrogen evolution and oxidation reactions. However, the commercial use of Pt as a cathode for water electrolysis is very limited because of its high cost. In addition to utilizing cheaper materials, such as Ni and Ni-based alloys, one way to overcome this problem is to develop a Pt electrode with a high specific surface area for catalytic reactions. Recently, nanostructured materials have attracted increasing attention because they may exhibit unusual physical and chemical properties that are significantly different from those of conventional bulk materials due to their extremely small size or large specific surface area.[1–3] Based on a reduction in the required Pt amount and the possible presence of special electrochemical properties, the development of Pt nanostructured electrodes becomes an important and interesting topic.[4,5]

Until now, only a few studies concerning the Pt nanostructured electrodes were reported; they were focused on glassy carbon-supported Pt (Pt/GC) nanostructured electrodes prepared by vacuum evaporation,[6] pulsed electrodeposition,[7] and electroplating.[8] The goal of these stuidies was to investigate the influence of the crystallite size and surface morphology on the intrinsic electrochemical properties, not to produce high-current-density electrodes. However, although these Pt/GC electrodes had high specific surface areas and provided valuable information, their current densities were low (i.e., several to several hundreds μA/cm^2 for hydrogen adsorption/desorption) because quite low loading of Pt was allowed. This revealed that a high specific surface area and a high current density are in contrast to each other for the development of electrodes. Recently, we proposed a new method to prepare a Pt/Ti nanostructured electrode by the electrophoretic deposition of Pt nanoparticles on a Ti support.[4,5] The resultant electrodes showed significantly higher current densities (i.e., several to several tens of mA/cm^2 for hydrogen adsorption/desorption) than did Pt/GC electrodes prepared by other methods, and hence should be more useful in practical applications.

Furthermore, it is known that the electrocatalytic activity of a Pt electrode can be modified by changing its surface composition with adatoms, such as Pd,[9–12] Bi,[13] Sb,[14] As,[15] and Ru.[16–22] Among them, Pt–Ru has received considerable attention because it is presently the best catalyst for the oxidation of methanol, and has great application possibilities in the development of fuel cells. To extend our previous work on the preparation of Pd and Pt nanoparticles[23,24] and a Pt/Ti nanostructured electrode,[4,5] in this work we further prepared a Pd-doped Pt/Ti nanostructured electrode by the electrophoretic co-deposition of Pt and Pd nanoparticles on a Ti support, and investigated the doping effect of Pd nanoparticles on the electrocatalytic activity for the oxidation of methanol. For Pt–Ru electrodes in fuel cells, the catalyst layer usually contained not only the Pt–Ru catalyst, but also carbon and Nafion (inert matrix). However, for the nanostructured electrode developed in this work, the catalyst layer was composed of only the catalysts itself. That is, the catalysts were deposited on the substrate surface, not embedded in an inert matrix. In addition, according to a study by Kadirgan et al.,[9] the Pd-doped Pt electrodes exhibited an enhanced electrocatalytic activity only in alkaline solutions. Also, a number of studies were performed in alkaline solutions[25–30] and it was found that some other metals were as active as Pt.[25,26,30] Accordingly, the electrocata-

lytic activity of a Pd-doped Pt nanostructured electrode was examined in an alkaline solution in this work.

Experimental

Materials. Hydrogen hexachloroplatinate(Ⅳ) hydrate was obtained from Acros Organics (Belgium). Palladium(Ⅱ) chloride, hydrazinium hydroxide, formic acid, and perchloric acid were guaranteed reagents of E. Merck (Darmstadt). Reagent-grade acetone and hydrochloric acid were supplied by Kanto Chemical Co. (Tokyo). Sodium di-2-ethylhexylsulfosuccinate (Aerosol OT), purchased from Sigma Chemical Co. (St. Louis, MO), was vacuum dried at 60 °C for 24 h and stored in a vacuum desiccator prior to use. HPLC-grade isooctane (2,2,4-trimethyl pentane), supplied by TEDIA (Fairfield), was dehydrated with molecular sieves 4Å (8–12 mesh, Janssen) for at least 24 h and kept in a vacuum desiccator before use. The residual water in an isooctane solution of Aerosol OT was recognized to be negligible using a Karl-Fisher moisture titrator (Kyoto Electronics MKC-500). The water used throughout this work was reagent-grade water produced by Milli-Q SP Ultra-Pure-Water Purification System of Nihon Millipore Ltd., Tokyo. Before use, Ti supports were first degreased with soap and water, then etched for 1 h in a 6.0 M HCl solution at 80–90 °C, ultrasonically cleaned with water and acetone, and finally dried in the atmosphere.

Preparation of Pd and Pt Nanoparticles. Pd and Pt nanoparticles were prepared in reverse micelles of water/Aerosol OT/isooctane at 25 °C according to our previous studies.[23,24] A reverse micellar solution containing $H_2[PtCl_6]$ (or $[Pd(NH_3)_4]Cl_2$) and hydrazine was prepared by injecting the required amounts of the corresponding aqueous solutions into an isooctane solution of Aerosol OT. By mixing equal volumes of two reverse micellar solutions at the same ω_0 ($[H_2O]/[\text{Aerosol OT}]$) value of 5 and an Aerosol OT concentration of 0.1 M, one containing an aqueous solution of 0.1 M $H_2[PtCl_6]$, and the other containing an aqueous solution of 1.0 M hydrazine, monodisperse Pt nanoparticles with a mean diameter of 7.4 nm could be obtained.[23] Similarly, at $[Pd(NH_3)_4Cl_2] = 0.05$ M and $\omega_0 = 10$, monodisperse Pd nanoparticles with a mean diameter of 16.5 nm were obtained.[24] Here, the concentration of Aerosol OT was based on the overall volume of the reverse micellar solution, while the concentrations of $H_2[PtCl_6]$ (or $[Pd(NH_3)_4]Cl_2$) and hydrazine were referred to the volume of an aqueous solution added into the reverse micellar solution.

Preparation of Nanostructured Electrode by Electrophoretically Co-deposition. Electrophoretic deposition was carried out at 25 °C with an 18-cm^3 reverse micellar solution containing the required Pt and Pd nanoparticles in a glass cell. The total catalyst loading (Pt and Pd) was fixed at 0.015 mmol/cm^2, referred to the geometric area. A Ti support and a Pt sheet were used as the cathode and anode, respectively. The spacing between the electrodes was 0.5 cm, and the geometric surface area of the Ti support for the co-deposition of Pt and Pd nanoparticles was 0.56 cm^2. During electrophoretic deposition, the solution gradually turned from dark brown to clear. It was found that the time required for the complete deposition of Pt and Pd nanoparticles onto the Ti support decreased with increasing the electric field strength or decreasing the total concentration of Pt and Pd nanoparticles. When the electric field strength was below 600 V/cm, the co-deposition of Pt and Pd nanoparticles onto the Ti support was quite insignificant, even after 8 h. However, when the electric field strength was above 1200 V/cm, the coagulation of metallic nanoparticles occurred in the solution. Therefore, an electric field strength of 1000 V/cm was used throughout this work. Under this condition, the time required for the complete deposition of Pt and Pd nanoparticles onto the Ti support was 1.5–3 h, increasing with an increase in the Pt content from 0 to 100%.

After deposition, the as-prepared electrode was removed from the solution and heated in air for 5 min to achieve the sintering of nanoparticles and to strengthen their bonding with the Ti support. If a heat treatment was not applied or the heat-treatment temperature was below 200 °C, the metallic nanoparticles would peel off the Ti support slightly. When the heat-treatment temperature was above 400 °C, the electrocatalytic activity of the resultant electrode decreased due to a significant sintering of the metallic nanoparticles. Hence, the heat treatment of the as-prepared electrodes was fixed at a temperature of 400 °C in this study.

Characterization. The surface morphology and elemental distribution of the resultant electrode were characterized using a scanning electron microscope (SEM) and a scanning electron microscopy-wavelength dispersive spectrometer (SEM-WDS) (Philips XL-40FEG), respectively. The crystal structure of the electrode was analyzed by a Rigaku D/max Ⅲ.Ⅴ X-ray diffractometer (XRD) using Cu Kα radiation ($\lambda = 0.1542$ nm).

The surface composition and electrocatalytic activity of the resultant electrodes were measured by cyclic voltammetry at 25 °C in a solution of 0.5 M H_2SO_4 and a mixed solution of 0.1 M CH_3OH and 1.0 M NaOH, respectively, using the Electrochemical Analyzer System, BAS CV-50W (Bioanalytic System, Inc.). Steady-state cyclic voltammograms were obtained after about twenty cycles. An Ag/AgCl electrode and a Pt wire were used as reference and counter electrodes, respectively. The tip of the reference electrode was set at a distance of 0.5 cm from the surface of the working electrode to minimize the error caused by the iR drop in the solution. Before a measurement, the solution was degassed with purified nitrogen gas for 15 min, and the working electrodes were polarized from 0 to 1.5 V at 100 mV/s for 10 min in a 0.5 M H_2SO_4 solution (for the determination of surface composition) or a 1.0 M NaOH solution (for the measurement of electrocatalytic activity). The sweep rate was fixed at 50 mV/s. The steady-state cyclic voltammograms were obtained after about twenty cycles. All of the potentials were given on a reversible hydrogen electrode (RHE) scale, and the current densities were values based on the geometric surface areas of the electrodes.

Results and Discussion

Surface Morphology and Elemental Distribution. Figure 1 shows typical SEM micrographs for the Pt/Ti, Pd-doped Pt/Ti, and Pd/Ti nanostructured electrodes. It was found that although the nanoparticles deposited on the Pt/Ti electrode remained discrete, serious sintering was observed for the Pd/Ti electrode. This might be due to the fact that Pd nanoparticles had a lower sintering temperature than Pt nanoparticles, as expected from their melting points at the bulk state (i.e., 1555 °C for Pd and 1773 °C for Pt). For nanoparticles on the Pd-doped Pt/Ti electrode, a slight sintering due to Pd nanoparticles was observed, but the nanostructure remained. In addition, from SEM-WDS micrographs (mapping) for the Pd-doped Pt electrode, as shown in Fig. 2, it could be seen that both Pt and Pd were uniformly deposited on the Ti support.

Crystal Structure. The typical XRD pattern of the resultant electrode is shown in Fig. 3. Although the characteristic

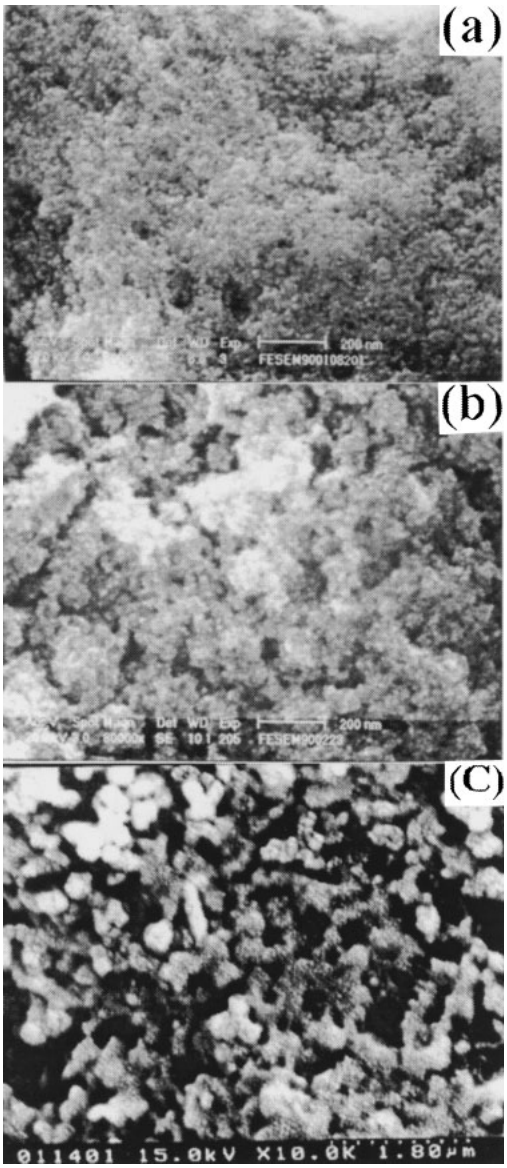

Fig. 1. SEM micrographs for a) Pt/Ti, b) Pd-doped Pt/Ti (Pd/Pt = 20/80 on the electrode surface), and c) Pd/Ti nanostructured electrodes.

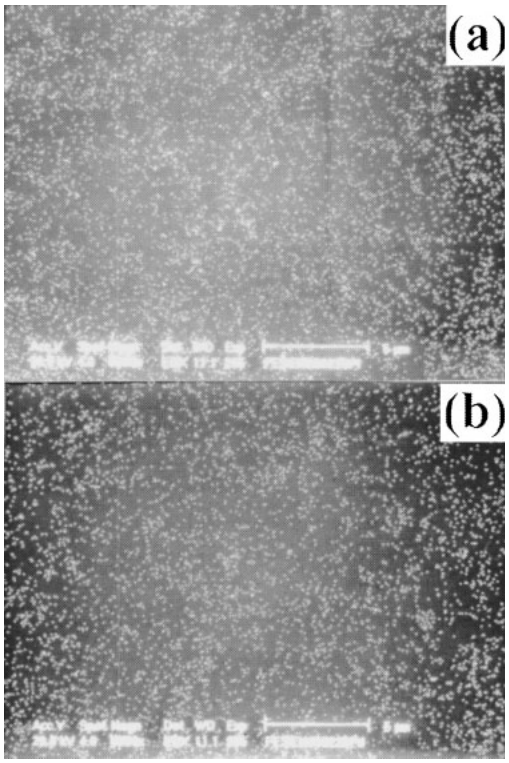

Fig. 2. SEM-WDS micrographs for the Pd-doped Pt/Ti nanostructured electrode (mapping). (a) Pt, (b) Pd (Pd/Pt = 20/80 on the electrode surface).

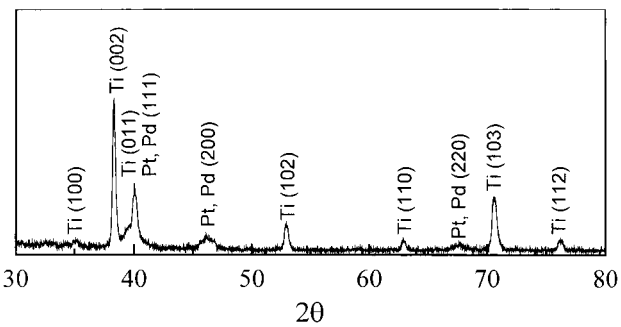

Fig. 3. XRD pattern of the Pd-doped Pt/Ti nanostructured electrode (Pt/Pd = 80/20 on the electrode surface).

peaks for Pt and those for Pd were too close to being distinguished, their characteristic peaks ($2\theta = 40$, 46, and 67°), indicated by their indices ((111), (200), and (220)), revealed that both Pt and Pd nanoparticles on the Ti support had a face-centered cubic (fcc) structure.

Surface Composition. Since electrocatalytic reactions usually occurred on the electrode surface, the surface compositions of the resultant electrodes should be examined. From typical steady-state cyclic voltammograms of the resultant electrodes in 0.5 M H_2SO_4, as shown in Fig. 4, it was found that the reduction peak (P) potential of the surface oxides for the Pd-doped Pt/Ti electrode was between those for the Pt/Ti and Pd/Ti electrodes. Assuming there was a linear relationship between the peak potentials of the surface oxides and the fractions of the two metals in the superficial layers,[9,12,31] the surface compositions of the Pd-doped Pt/Ti electrodes with various Pd/Pt ratios could be estimated by interpolating their peak potentials. As shown in Fig. 5, the Pd contents on the electrode surfaces were lower than those in electrodeposition solutions. This could be attributed to the faster deposition rate of Pd nanoparticles than Pt nanoparticles.

Electrocatalytic Activity. Figure 6 shows steady-state cyclic voltammograms for the resultant electrodes in a mixed solution of 0.1 M CH_3OH and 1.0 M NaOH. Their features are essentially similar, except that the current density of the Pd/Ti electrode was significantly lower than others because Pd was relatively inactive for the oxidation of methanol.

According to previous studies on conventional Pd/Pt alloy electrodes,[15,16,32–36] the mechanism for the oxidation of methanol could be formulated as follows:

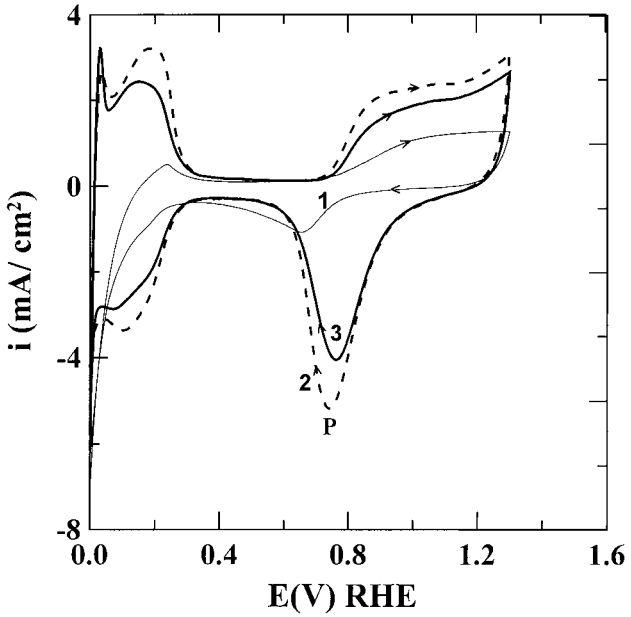

Fig. 4. Steady-state cyclic voltammograms for 1) Pd/Ti, 2) Pd-doped Pt/Ti (Pt/Pd = 80/20 on the electrode surface), and 3) Pt/Ti nanostructured electrodes in 0.5 M H_2SO_4 solution.

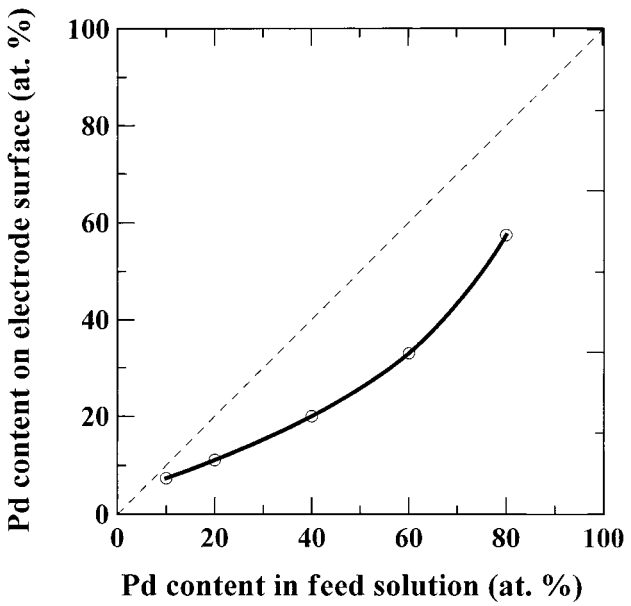

Fig. 5. A plot of the surface composition of Pd-doped Pt/Ti nanostructured electrode against the composition in electrodeposition solution.

$$CH_3OH_{sol} = CH_3OH_{ads}, \quad (1)$$

$$CH_3OH_{ads} \rightarrow CO_{ads} + 4H^+ + 4e^-, \quad (2)$$

$$H_2O = OH_{ads} + H^+ + e^- \quad \text{(on Pd)}, \quad (3)$$

$$H_2O = OH_{ads} + H^+ + e^- \quad \text{(on Pt)}, \quad (4)$$

$$CO_{ads} + OH_{ads} \rightarrow CO_2 + H^+ + e^-. \quad (5)$$

Methanol first adsorbed and dissociated on the electrode surface to form the main intermediate, CO_{ads}.[29] Then, CO_{ads} was oxidized by OH_{ads} via reaction 5 at peak P_1 (0.87 V) in a positive-going scan and at peak P_2 (0.72 V) in a negative-going scan. Plots of the onset potential and current density at 0.7 V for methanol oxidation against the Pd content on electrode surface are shown in Figs. 7 and 8, respectively. With increasing the Pd content on the electrode surface, the onset potential for methanol oxidation first decreased and then increased, while the current density first increased and then decreased after reaching a minimum at a surface composition of 20 atom % Pd. This revealed that the doping of an appropriate amount of Pd nanoparticles could enhance the electrocatalytic activity of the Pt electrode. Although Pd is less active than Pt for reaction 1, the rate of reaction 3 is higher than that of reaction 4 since the binding energy of water for Pd is higher than that for Pt.[36] Therefore, the doping of Pd caused a faster formation of OH_{ads} by reaction 3, and led to an increase in the

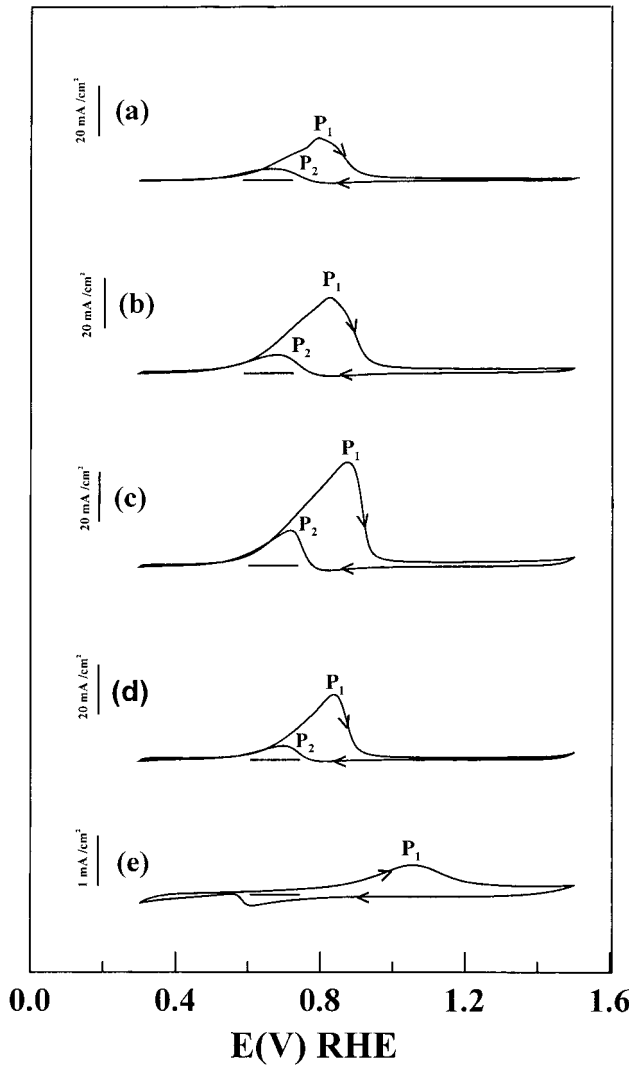

Fig. 6. Steady-state cyclic voltammograms in a mixed solution of 0.1 M CH_3OH and 1.0 M NaOH for a) Pt/Ti, b) Pd-doped Pt/Ti (Pt/Pd = 92.6/7.4 on the electrode surface), c) Pd-doped Pt/Ti (Pt/Pd = 80/20 on the electrode surface), d) Pd-doped Pt/Ti (Pt/Pd = 42.6/57.4 on the electrode surface), and (e) Pd/Ti nanostructured electrodes.

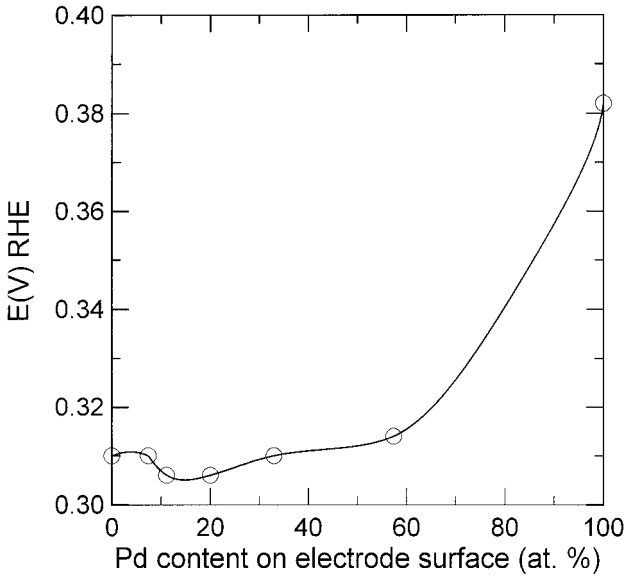

Fig. 7. A plot of onset potential for methanol oxidation against the surface compositions of Pd-doped Pt/Ti nanostructured electrodes.

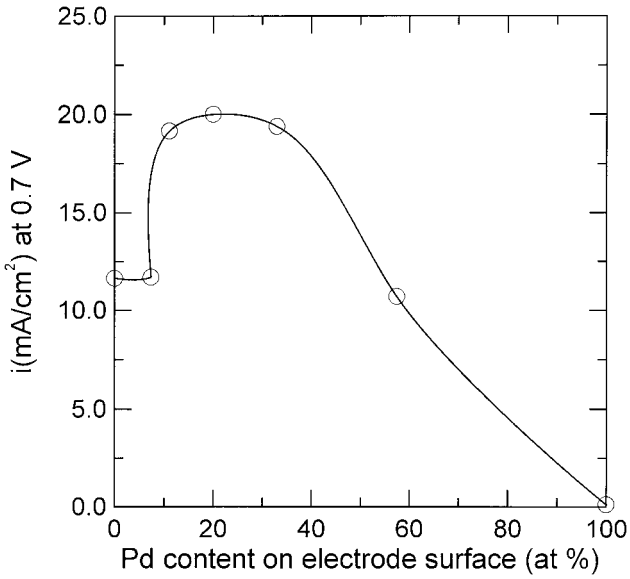

Fig. 8. A plot of current density for methanol oxidation at 0.7 V against the surface compositions of Pd-doped Pt/Ti nanostructured electrodes.

rates of reaction 5 and the overall reaction. As for the decreased electrocatalytic activity at a high Pd content, it was reasonably referred to the fact that most sites for reaction 1 were occupied by Pd, leading to a decrease in the rate of reaction 1 and the overall reaction. The activity enhancement of Pd-doped Pt electrodes was consistent with the results observed in the cases of conventional Pd–Pt alloy electrodes.[9–12] However, although the Pd-doped Pt electrode obtained in this work had a significantly higher electrocatalytic activity due to its nanostructure, its activity enhancement was lower than that of the conventional Pd–Pt alloy electrodes. This might be because the Pd-doped Pt electrode was prepared from preformed Pt and Pd nanoparticles, and hence its composition distribution was not as homogeneous as conventional Pd/Pt alloy electrodes.

It is noted that the electrodes were prepared using individual Pt and Pd nanopartilces in this work. Since the heat-treatment temperature was only 400 °C, an alloy of Pt and Pd might not have been formed. That is, the doping of Pd within the Pt layer was not at the atomic level. This implied that the nanoparticle-deposited electrodes also might have exhibited a similar behavior as did alloy electrodes. Since the internal structure and property of nanoparticles might be affected by their interaction,[1–3] it was suggested that the activity enhancement or diminution resulted from the doping of Pd atoms in bulk Pt might also be achieved via an interaction between Pt and Pd nanoparticles. More detailed studies are necessary in the future.

In this work, a novel Pd-doped Pt/Ti nanostructured electrode prepared by the electrophoretically co-deposition of Pt and Pd nanoparticles had an appropriately high current density and specific activity. Such bimetallic nanostructured electrodes have not been reported until now. In addition, it is known that increasing the temperature can greatly enhance the current densities of fuel cells.[16] According to studies of Gasteiger et al.,[16] the current density of a Pt–Ru electrode increased by about 10-fold while increasing the temperature from 25 to 60 °C. Therefore, recent fuel cells using Pt–Ru catalyst are usually operated at higher temperatures (e.g., 60–130 °C)[16–22] to obtain high current densities. For example, in a study of Küver and Vielstich,[21] when Pt–Ru loading was 2.3 mg/cm^2, the current density at 100 °C was 100 mA/cm^2. In this work, when a Pt–Pd electrode was used at an overall composition of 40 atom% Pd (i.e., surface composition = 20 atom% Pd), the Pt–Pd loading was 2.4 mg/cm^2 (Pt: 1.76 mg, Pd: 0.64 mg) and the current density at 25 °C was 55 mA/cm^2. (Note that the data mentioned here refer to the geometric area.) Although a lower current density was obtained at a similar catalyst loading, the Pt–Pd electrode developed in this work was operated at 25 °C, and might exhibit a higher current density at higher temperatures. This revealed that the Pd-doped nanostructured electrode developed in this work and the recent Pt–Ru electrode for fuel cells are comparable. Furthermore, at a surface composition of 20 atom% Pd, the current density at 25 °C was 55 mA/cm^2. This reveals that the resultant electrode had a rather high current density and specific activity, and might be useful in the development of micro-fuel cells for various kinds of electronic products performed at room temperature.

Conclusion

A novel Pd-doped Pt/Ti nanostructured electrode was successfully prepared by the electrophoretic co-deposition of Pt and Pd nanoparticles on a Ti support. The total catalyst loading (Pt and Pd) was fixed at 0.015 mmol/cm^2, referred to the geometric area. Analyses of SEM and SEM-WDS revealed that Pd and Pt nanoparticles were uniformly deposited and remained discrete on the Ti support, although a slight sintering was observed in the presence of Pd. Also, from the XRD pattern, it was found that both Pt and Pd nanoparticles deposited on the electrode had a fcc structure. From electrochemical

measurements, the surface compositions of the Pd-doped Pt/Ti electrodes with various Pd/Pt ratios were estimated and controlled by adjusting the compositions of the electrodeposition solutions. With increasing the Pd content on the electrode surface, the Pd-doped Pt/Ti electrode exhibited a maximum electrocatalytic activity at a surface composition of 20 atom % Pd and a lower activity than did the Pt/Ti electrode at a surface composition above 60 atom % Pd for the oxidation of CH_3OH. It revealed that the interaction between Pt and Pd nanoparticles could cause an enhancement or diminution of the electrocatalytic activity, like that observed in the case of conventional alloy electrodes. Furthermore, the current density was 55 mA/cm^2 at 25 °C and a surface composition of 20 atom % Pd, revealing that the resultant electrode had a rather high current density and specific activity. This work provides a new method to enhance the electrocatalytic activity by the doping of a second metal, and should be helpful for the developments of Pt nanostructured electrodes and micro-fuel cells.

This work was performed under the auspices of the National Science Council of the Republic of China, under contract number NSC 87-2214-E006-010, to which the authors express their thanks.

References

1 C. Hayashi, *Phys. Today*, **40**, 44 (1987).
2 H. Gleiter, *Prog. Mater. Sci.*, **33**, 223 (1989).
3 R. Uyeda, *Prog. Mater. Sci.*, **35**, 1 (1991).
4 L. B. Lai, D. H. Chen, and T. C. Huang, *Mater. Res. Bull.*, **36**, 1049 (2001).
5 L. B. Lai, D. H. Chen, and T. C. Huang, *J. Mater. Chem.*, **11**, 1491 (2001).
6 Y. Takasu, Y. Fujii, K. Yasuda, Y. Iwanaga, and Y. Matsua, *Electrochim. Acta*, **34**, 453 (1989).
7 J. L. Zubimendi, G. Andreasen, and W. E. Triaca, *Electrochim. Acta*, **40**, 1305 (1995).
8 P. Stonehart and J. Lundquist, *Electrochim. Acta*, **18**, 907 (1973).
9 F. Kadirgan, B. Beden, J. M. Leger, and C. Lamy, *J. Electroanal. Chem.*, **125**, 89 (1981).
10 G. A. Attard and A. Bannister, *J. Electroanal. Chem.*, **300**, 467 (1991).
11 M. J. Llorca, J. M. Feliu, A. Aldaz, and J. Clavilier, *J. Electroanal. Chem.*, **376**, 151 (1994).
12 A. Capon and R. Parsons, *J. Electroanal. Chem.*, **65**, 285 (1975).
13 J. Clavilier, A. Fernandez-Vega, J. M. Feliu, and A. Aldaz, *J. Electroanal. Chem.*, **258**, 89 (1989).
14 A. Fernandez-Vega, J. M. Feliu, A. Aldaz, and J. Clavilier, *J. Electroanal. Chem.*, **258**, 101 (1989).
15 A. Fernandez-Vega, J. M. Feliu, A. Aldaz, and J. Clavilier, *J. Electroanal. Chem.*, **305**, 229 (1991).
16 H. A. Gasteiger, N. Marković, Jr., P. N. Ross, and E. J. Cairns, *J. Electrochem. Soc.*, **141**, 1795 (1994).
17 S. Wasmus and A. Küver, *J. Electroanal. Chem.*, **461**, 14 (1999).
18 A. K. Shukla, P. A. Christensen, A. Hamnett, and M. P. Hogarth, *J. Power Sources*, **55**, 87 (1995).
19 M. Waidhas, W. Drenckhahn, W. Preidel, and H. Landes, *J. Power Sources*, **61**, 91 (1996).
20 J. Cruickshank and K. Scott, *J. Power Sources*, **70**, 40 (1998).
21 A. Küver and W. Vielstich, *J. Power Sources*, **74**, 211 (1998).
22 A. Heinzel and V. M. Barragán, *J. Power Sources*, **84**, 70 (1999).
23 D. H. Chen, J. J. Yeh, and T. C. Huang, *J. Colloid Interface Sci.*, **215**, 159 (1999).
24 D. H. Chen, C. C. Wang, and T. C. Huang, *J. Colloid Interface Sci.*, **210**, 123 (1999).
25 M. Beltowska-Brzezinska and I. Heibaum, *J. Electroanal. Chem.*, **183**, 167 (1985).
26 K. Machida and M. Enyo, *Bull. Chem. Soc. Jpn.*, **58**, 2043 (1985).
27 F. Hahn, B. Beden, and C. Lamy, *J. Electroanal. Chem.*, **204**, 315 (1986).
28 O. Enea, *Electroanal. Chem.*, **235**, 393 (1987).
29 G. Kokkinidis and D. Jannakoudakis, *J. Electroanal. Chem.*, **153**, 185 (1983).
30 K. Machida, K. Nishimura, and M. Enyo, *J. Electrochem. Soc.*, **133**, 2522 (1986).
31 N. R. de Tacconi, J. M. Leger, B. Beden, and C. Lamy, *J. Electroanal. Chem.*, **134**, 117 (1982).
32 S. Wilhelm, T. Iwasita, and W. Vielstich, *J. Electroanal. Chem.*, **238**, 383 (1987).
33 T. Iwasita, E. Santos, and W. Vielstich, *J. Electroanal. Chem.*, **229**, 367 (1987).
34 T. Iwasita and U. Vogel, *Electrochim. Acta*, **33**, 560 (1988).
35 H. Kita and H. W. Lei, *J. Electroanal. Chem.*, **388**, 167 (1995).
36 A. B. Anderson, E. Grantscharova, and S. Seong, *J. Electrochem. Soc.*, **143**, 2075 (1996).